NIH Public Access
Author Manuscript
Nature. Author manuscript; available in PMC 2012 January 30.

Published in final edited form as:
Nature. ; 475(7357): 497–500. doi:10.1038/nature10214.

A role for glia in the progression of Rett syndrome

Daniel T. Lioy[1,6,12], **Saurabh K. Garg**[1,6,12], **Caitlin E. Monaghan**[1,6,12], **Jacob Raber**[2,3,6], **Kevin D. Foust**[7], **Brian K. Kaspar**[7], **Petra G. Hirrlinger**[8], **Frank Kirchhoff**[9,10], **John M. Bissonnette**[4,5,6], **Nurit Ballas**[11], and **Gail Mandel**[1,6,12,*]

[1]Vollum Institute, Portland, Oregon

[2]Departments of Behavioral Neuroscience and Neurology, Portland, Oregon

[3]Division of Neuroscience, ONPRC, Portland, Oregon

[4]Department of Cell and Developmental Biology, Portland, Oregon

[5]Department of Obstetrics and Gynecology, Portland, Oregon

[6]Oregon Health and Science University, Portland, Oregon

[7]Department of Pediatrics, The Ohio State University, Center for Gene Therapy, Nationwide Children's Hospital, Columbus, Ohio

[8]Paul-Flechsig-Institute for Brain Research, Leipzig, Germany

[9]Department of Neurogenetics, Max Planck Institute of Experimental Medicine, Gottingen, Germany

[10]Institute of Physiology, University of Saarland, Homburg, Germany

[11]Department of Biochemistry and Cell Biology, State University of New York, Stony Brook

[12]Howard Hughes Medical Institute.

Abstract

Rett syndrome (RTT) is an X-chromosome-linked autism spectrum disorder caused by loss of function of the transcription factor methyl CpG-binding protein 2 (MeCP2)[1]. Although MeCP2 is expressed in most tissues[2], loss of MeCP2 results primarily in neurological symptoms[1,3,4]. Earlier studies propelled the idea that RTT is due exclusively to loss of MeCP2 function in neurons[2,4-10]. While defective neurons clearly underlie the aberrant behaviors, we and others showed recently that the loss of MeCP2 from glia negatively influences neurons in a non-cell autonomous fashion[11-13]. Here, we show that in globally MeCP2-deficient mice, re-expression of MeCP2 preferentially in astrocytes significantly improved locomotion and anxiety levels, restored respiratory abnormalities to a normal pattern, and greatly prolonged lifespan compared to globally null mice. Furthermore, restoration of MeCP2 in the mutant astrocytes exerted a non-cell-autonomous positive effect on mutant neurons *in vivo*, restoring normal dendritic morphology and increasing levels of the excitatory glutamate transporter (VGlut1). Our study shows that glia, like neurons, are integral components of the neuropathology of RTT, and supports targeting glia as a strategy for improving the associated symptoms.

* Corresponding author: mandelg@ohsu.edu.

Author contributions D. T. L., S. K. G., J. R., J. M. B., N. B., and G. M. designed the astrocyte knockout and rescue experiments. B. K. K. and K. D. F. helped design the AAV9 experiments. D. T. L., S. K. G., C. E. M., and J. M. B. performed the experiments. P. G. H. and F. K. provided the *hGFAPcreT2* transgenic mice. D. T. L., S. K. G., N. B., and G. M. wrote the manuscript with input from the other co-authors.

NIH-PA Author Manuscript
NIH-PA Author Manuscript
NIH-PA Author Manuscript

NIH-PA Author Manuscript

NIH-PA Author Manuscript

NIH-PA Author Manuscript

Global re-expression of MeCP2 postnatally in MeCP2-deficient mice allows normal longevity, rescues motor behaviors, and improves overall health[14]. Because expression of MeCP2 from the neuronal *tau* locus in early development prevents appearance of several RTT-like symptoms[9], neurons are likely crucial components in a rescue. However, prior *in vitro* studies indicate that astrocytic MeCP2 supports normal neuronal morphology[11,12]. Therefore, we asked whether astrocytes might also play a role in rescuing RTT neuropathology *in vivo*.

To this end, we crossed mice harboring a tamoxifen (TAM)-inducible cre recombinase transgene driven by the human astrocytic glial fibrillary acidic protein (*hGFAP*) promotor[15] (also see Ref. 16 - 18), with mice containing a cre-excisable transcriptional *stop* sequence in the endogenous *Mecp2* gene (*Mecp2*^{Stop})[14]. The progeny that inherited both alleles are referred to as *Mecp2*^{Stop}-*hGFAP*creT2 mice (Supplemantary Fig. 1a). We determined the efficiency of astrocytic excision in ROSA-reporter[15] and *Mecp2*$^{Stop/y}$-*hGFAPcreT2* mice (Supplementary Fig. 1b, c, and d). The percentage of MeCP2^{+} / GFAP^{+} astrocytes was extremely high in caudal brain regions[15], similar to *Mecp2*$^{+/y}$ (Fig. 1a and Supplementary Fig. 1e). Re-expression of MeCP2 was not detected in oil-treated *Mecp2*$^{Stop/y}$-*hGFAPcreT2* mice (Supplementary Fig. 2a). Importantly, only a very low percentage (< 5%) of excision in neurons was detected by immunolabeling, PCR analysis of the recombined *stop* sequence, and single cell immunofluorescence intensity measurements (Fig. 1 and Supplementary Figs. 1f and g and 3). This low percentage did not increase with age (Supplementary Figs. 1g and 4), and MeCP2 re-expression was restricted to brain (Supplementary Fig. 5c). Over-expression of MeCP2 in rescued astrocytes was not observed (Supplementary Fig. 2b).

To rule out that the small percentage of neurons, in combination with the low constitutive level of MeCP2 in the *stop* mice (Supplemental Fig. 5b and c), might mediate any behavioral changes we would measure, we systemically injected young male *Mecp2*$^{Stop/y}$ mice with a suboptimal titer of recombinant MeCP2-AAV9 virus[19] or virus lacking MeCP2. This resulted in physiological levels of MeCP2 expression in 2% to 35% of neurons, depending on the brain region (Supplementary Fig. 6a - c). Regardless of genotype, none of the treated mice showed improvement of RTT-like phenotypes compared to the control-AAV9 injected *Mecp2*$^{-/y}$ mice (Supplementary Fig. 6d - g). Taken together, the results validate the use of the *hGFAPcreT2* system for dissecting astrocytic contributions to RTT.

The average lifespan of oil-treated *Mecp2*$^{Stop/y}$-*hGFAPcreT2* and *Mecp2*$^{Stop/y}$ mice was only three months[14], which is prolonged compared to *Mecp2*$^{-/y}$ mice[3,4] (Supplementary Fig. 5a), and likely due to the small amount of MeCP2 protein expressed from the *stop* locus (Supplementary Fig. 5b and c). In contrast, nine of 11 TAM-treated *Mecp2*$^{Stop/y}$-*hGFAPcreT2* mice were alive at 7.5 months, when seven of the nine were sacrificed for further analysis. The longest living mouse was sacrificed at 15 months. The TAM-treated *MeCP2*$^{Stop/y}$-*hGFAPcreT2* mice were also on average 20% larger than oil-treated *MeCP2*$^{Stop/y}$-*hGFAPcreT2* mice (Supplementary Fig. 7a). Using a previously described observational scoring system[14], overall health of the TAM-treated male (Supplementary Fig. 7b) and female (Supplementary Fig. 8) mice stabilized, rather than worsened like the oil-treated controls, and TAM treatment of a highly symptomatic *MeCP2*$^{Stop/y}$-*hGFAPcreT2* mouse reversed symptoms to nearly *hGFAPcreT2* values (Supplementary Fig. 9, Videos S1 and S2).

MeCP2-deficient mice are hypoactive[1,3,4] and show altered measures of anxiety-related behaviors[6]. In the home cage (Fig. 2a and b) and open field (Fig. 2c), oil-treated *Mecp2*$^{Stop/y}$-*hGFAPcreT2* mice traveled only ~20% the distance, and did so at ~20% the velocity, of *hGFAPcreT2* control mice. TAM-treated *Mecp2*$^{Stop/y}$-*hGFAPcreT2* mice, however, improved to ~50% the level of *hGFAPcreT2* mice in both measures. Similar

NIH-PA Author Manuscript

NIH-PA Author Manuscript

NIH-PA Author Manuscript

improvements were observed in an open field test to measure anxiety. The oil-treated *Mecp2*$^{Stop/y}$*-hGFAPcreT2* mice spent only ~20% as much time in the center of the cage as *hGFAPcreT2* mice, while TAM-treated *Mecp2*$^{Stop/y}$*-hGFAPcreT2* mice again improved to ~50% the level of *hGFAPcreT2* mice (Fig. 2d). The ratio of distance traveled in the center square to total distance was the same for all genotypes (data not shown). In the elevated zero and plus mazes, *Mecp2*$^{-/y}$ mice consistently show decreased anxiety-related behavior[20,21]. The TAM-treated *Mecp2*$^{Stop/y}$*-hGFAPcreT2* mice were more anxious than the oil-treated *Mecp2*$^{Stop/y}$*-hGFAPcreT2* mice in the elevated zero maze, improving up to ~50% the level of the control *hGFAPcreT2* mice (Fig. 2e)

RTT patients and mouse models have abnormal respiration[1,22] (Fig. 3a). By 12 weeks, *Mecp2*$^{Stop/y}$*-hGFAPcreT2* mice had irregularity scores and apnea rates significantly more severe than *hGFAPcreT2* controls (Fig. 3a and b and Supplementary Fig. 7c, Traces 1 and 2). In contrast, two months after TAM-treatment, the respiratory pattern in 10 of 12 *Mecp2*$^{Stop/y}$*-hGFAPcreT2* mice were within normal range (Fig. 3b). Two mice followed over the subsequent five-month period maintained a regular breathing patterns (data not shown). In two of three TAM-treated mice, we observed complete reversal to a normal respiratory pattern (Fig. 3a and Supplementary Fig. 7c, Traces 3 and 4). The apneic frequency in the third mouse was reduced but did not completely reverse to control levels (Supplementary Fig. 7c, Trace 5). The improvement in respiration was consistent with efficient re-expression of MeCP2 in GFAP^{+} astrocytes within the preBötzinger complex of the brainstem, an area implicated in respiratory defects in RTT[23] (Supplementry Fig. 7e). Treatment of a *Mecp2*$^{Stop/y}$ mouse with TAM did not alleviate the irregular breathing or apneic frequency (Supplementary Fig. 7c, Trace 2). Oil-treated female *Mecp2*$^{+/Stop}$*-hGFAPcreT2* mice developed a significant number of apneas beginning at four to six months (Fig. 3c). The apneic breathing was corrected by TAM treatment (Fig. 3c), even in the most severely affected female (Supplementary Fig. 7d).

The brains of girls with RTT and affected mice exhibit smaller neuronal somal sizes and reduced dendritic complexity in some regions[1,4,24,25]. At ~ 3.5 months of age, the somal sizes of neurons in hippocampus, cerebellum, and cortex were still smaller in TAM-treated *Mecp2*$^{Stop/y}$*-hGFAPcreT2* mice compared to *hGFAPcreT2* controls. At seven months, however, somal size was restored only in brain regions showing astrocytic re-expression of MeCP2 (Fig. 4a). Regarding dendritic complexity, the *Mecp2*$^{Stop/y}$ and oil- treated *Mecp2*$^{Stop/y}$*-hGFAPcreT2* mice had ~25% fewer total number of apical dendrite branches compared to controls. By 3.5 months of age, however, neurons in TAM-treated *Mecp2*$^{Stop/y}$*-hGFAPcreT2* mice had a normal number of branches and this was sustained with further age (Fig. 4b and c). MeCP2-deficient neurons also show deficits in proteins necessary for excitatory neurotransmission, such as VGlut1[26,27]. We detected ~20% fewer peri-nuclear VGlut1^{+} puncta in *Mecp2*$^{Stop/y}$ and oil-treated *Mecp2*$^{Stop/y}$*-hGFAPcreT2* mice compared to controls, but the levels increased to normal by three to four months of age with TAM-treatment of *Mecp2*$^{Stop/y}$*-hGFAPcreT2* mice (Fig. 4d and e). Taken together, the anatomical findings suggest that re-expression of MeCP2 in astrocytes can, through a non-cell autonomous mechanism, positively influence components of the neurotransmission machinery *in vivo*.

Our results show that re-expression of MeCP2 in astrocytes ameliorates overt RTT-like phenotypes in mice. To address the complementary question of the consequences of the removal of MeCP2 from astrocytes, we crossed mice with a floxed MeCP2 allele[4] to the same *hGFAPcreT2*[15] line used for the rescue. Recombination efficiencies throughout the brain were again higher in caudal compared to rostral regions (Supplementary Fig. 10a and b). The knockout progeny displayed some phenotypes shared with null MeCP2 mice, such as smaller body size, clasped hindlimb posture, and irregular breathing (Supplementary Fig.

NIH-PA Author Manuscript

NIH-PA Author Manuscript

NIH-PA Author Manuscript

10c, d, and f), but their lifespans, locomotion (data not shown), and anxiety-related behaviors were all normal (Supplementary Fig. 10e). Further, loss of MeCP2 from astrocytes did not affect the number of CA1 apical dendritic branches (Supplementary Fig. 10g). This suggests that loss of MeCP2 in astrocytes at postnatal day 21 is unable to disrupt the already established hippocampal neuronal circuitry. In contrast, loss from and gain of MeCP2 in astrocytes resulted in a strong non-cell autonomous influence on breathing pattern. Thus, distinct neuronal-glial interactions may underlie hippocampal and hindbrain breathing circuitries.

Our results indicate that RTT involves impairments in both neurons and glia. In familial amyotrophic lateral sclerosis[28], neurons and glia are proposed to play different roles in the disease process, with neurons primarily initiating the disease and astrocytes primarily affecting disease progression. Our results are compatible with this model, because removal of MeCP2 just from astrocytes, at postnatal day 21, results in a subtler phenotype than the global null, and re-expression in astrocytes mainly stabilizes symptoms. Along these lines, the appearance of a subset of phenotypes after embryonic removal of MeCP2 from subsets of neurons[4,6-10,29] could be explained by causing disease initiation, and prevention of RTT-like phenotypes after MeCP2 re-expression in embryonic neurons[9] could be interpreted as preventing disease initiation. None of these studies address whether it could take both MeCP2-deficient neurons and glia to cause disease progression, or whether other non-neuronal cell types, including other glial types, might be involved in the disease process.

In sum, although impaired neurons ultimately underlie nervous system failure in RTT, restoring MeCP2 in glia can ameliorate four consistent and robust features of mouse models of RTT: premature lethality, aberrant respiration, hypoactivity, and decreased dendritic complexity. Future studies identifying the key molecules that are restored after glial MeCP2 re-expression may provide further clues into the mechanism of recovery, thereby providing new potential targets for therapeutic intervention.

Methods summary

Male mice harboring an *hGFAPcreERT2* transgene were crossed to female *Mecp2*$^{+/Stop}$ or *Mecp2*$^{+/Jaenisch.Flox}$ mice and the F1 progeny were injected with 100mg/kg tamoxifen or oil when appropriate. Mice used in astrocyte-rescue experiments were backcrossed for at least seven generations to a C57BL6 background. Mice used in astrocyte-knockout experiments were of a FVB/N/C57BL6 background. Histology was performed on transcardially perfused, frozen sections. Behavior was analyzed using CleverSystems StereoScan software. Body plethysmography was performed on unanesthetized restrained mice. Statistics were performed with Graphpad PRISM V5.0C software. Mouse maintenance, breeding, and genotyping, tamoxifen treatments, phenotype scoring, tissue preparation and immunohistochemistry, fluorescence intensity measurements, FACS, plethysmography, motor activity and anxiety assessments, western blotting, and statistics were performed as described in Supplementary Methods.

Supplementary Material

Refer to Web version on PubMed Central for supplementary material.

Acknowledgments

We thank P. Brehm, R. H. Goodman, C. Bond, M. McGinley, and C. Mandel-Brehm for helpful discussions, P. Micha, J. Eng, S. Knopp, and T. Shaffer for technical support, and M. Murtha for generating the CBA/CMV-MeCP2 construct. ViraPur, LLC generated the AAV9 virus. The work was supported by grants from the National Institutes of Health (G. M and N. B.), International Rett Syndrome Foundation (N. B. and J. M. B.), Rett Syndrome

NIH-PA Author Manuscript

NIH-PA Author Manuscript

NIH-PA Author Manuscript

Research Trust (G. M. and B. K. K.), Oregon Brain Institute (D. T. L.), and OHSU Cell and Developmental Biology Training Program (D. T. L.). Gail Mandel is an Investigator of the Howard Hughes Medical Institute.

References

1. Chahrour M, Zoghbi HY. Neuron. 2007; 56:422–37. [PubMed: 17988628]
2. Shahbazian MD, Antalffy B, Armstrong DL, Zoghbi HY. Hum. Mol. Genet. 2002; 11:115. [PubMed: 11809720]
3. Guy J, Hendrich B, Holmes M, Martin JE, Bird A. Nat. Genet. 2001; 3:322–6. [PubMed: 11242117]
4. Chen RZ, Akbarian S, Tudor M, Jaenisch R. Nat. Genet. 2001; 3:327–31. [PubMed: 11242118]
5. Kishi N, Macklis JD. Mol. Cell Neurosci. 2004; 27:306–21. [PubMed: 15519245]
6. McGill BE, Bundle SF, Yaylaoglu MB, Carson JP, Thaller C, Zoghbi HY. PNAS. 2006; 103:18267–72. [PubMed: 17108082]
7. Fyffe SL, et al. Neuron. 2008; 59:947–58. [PubMed: 18817733]
8. Samaco RC, et al. PNAS. 2009; 106:21966–71. [PubMed: 20007372]
9. Luikenhuis S, Giacometti E, Beard CF, Jaenisch R. PNAS. 2004; 101:6033–8. [PubMed: 15069197]
10. Chao HT, et al. Nature. 2010; 468:263–9. [PubMed: 21068835]
11. Ballas N, Lioy DT, Grunseich C, Mandel G. Nat. Neurosci. 2009; 12:311–7. [PubMed: 19234456]
12. Maezawa I, Swanberg S, Harvey D, LaSalle JM, Jin LW. J. Neurosci. 2009; 29:5051–61. [PubMed: 19386901]
13. Maezawa I, Jin LW. J. Neurosci. 2010; 30:5346–56. [PubMed: 20392956]
14. Guy J, Gan J, Selfridge J, Cobb S, Bird A. Science. 2007; 315:1143–7. [PubMed: 17289941]
15. Hirrlinger PG, Scheller A, Braun C, Hirrlinger J, Kirchhoff F. Glia. 2006; 54:11–20. [PubMed: 16575885]
16. Brenner M, Kisseberth WC, Su Y, Besnard F, Messing A. J. Neurosci. 1994; 14:1030–7. [PubMed: 8120611]
17. Chow L, Zhang J, Baker SJ. Transgenic Res. 2008; 17:919–28. [PubMed: 18483774]
18. Casper KB, Jones K, McCarthy KD. Genesis. 2007; 45:292–9. [PubMed: 17457931]
19. Foust KD, Nurre E, Montgomery CL, Hernandez A, Chan CM, Kaspar BK. Nat. Biotechnol. 2008; 27:59–65. [PubMed: 19098898]
20. Stearns NA, Schaevitz LR, Bowling H, Nag N, Berger UV, Berger-Sweeney J. Neurosci. 2007; 146:907–21.
21. Pelka GJ, et al. Brain. 2006; 129(Pt. 887-98)
22. Weese-Mayer DE, et al. Pediatr. Res. 2006; 60:443–9. [PubMed: 16940240]
23. Viemari J, et al. J. Neurosci. 2005; 25:11521–30. [PubMed: 16354910]
24. Bauman ML, Kemper TL, Arin DM. Neurol. 1995; 45:1581–6.
25. Armstrong DD. J. Child Neurol. 2005; 20:747–53. [PubMed: 16225830]
26. Chao HT, Zoghbi HY, Rosenmund C. Neuron. 2007; 56:58–65. [PubMed: 17920015]
27. Marchetto ML. Cell. 2010; 143:527–39. [PubMed: 21074045]
28. Ilieva H, Polymenidou M, Cleveland DW. J. Cell Biol. 2009; 187:761–72. [PubMed: 19951898]
29. Gemelli T, Berton O, Nelson ED, Perrotti LI, Jaenisch R, Monteggia LM. Biol. Psych. 2006; 59:468–76.

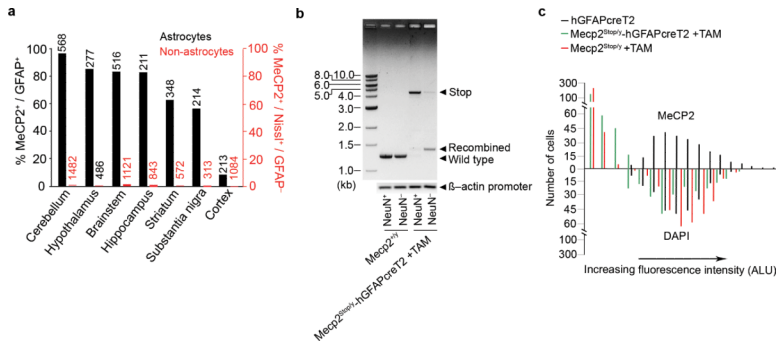

Figure 1.

a, Efficiencies of *Mecp2* re-expression. The numbers above the bars indicate total number of cells counted. **b**, Genomic PCR analysis of non-recombined (Stop; 4.3 kb) and recombined amplicons (1.29 kb) of FACS-sorted $NeuN^+$ and $NeuN^-$ cells from the whole brain of a TAM-treated *Mecp2*$^{Stop/y}$*-hGFAPcreT2* mouse. Genomic DNA was prepared from 500,000 cells per group. The wild-type (1.25 kb) *Mecp2* amplicon is indicated. The β-actin promoter amplicon shows that similar amounts of DNA were present in the reactions. **c**, Fluorescence-intensity histogram derived from individual hippocampal pyramidal neurons in tissue sections. Cy2 immunofluorescence intensities of nuclear MeCP2 protein are indicated above the line; DAPI fluorescence intensities of the same neurons are indicated below the line. ALU, arbitrary linear units. *n* = 3 mice per genotype and 100 cells per mouse.

NIH-PA Author Manuscript NIH-PA Author Manuscript NIH-PA Author Manuscript

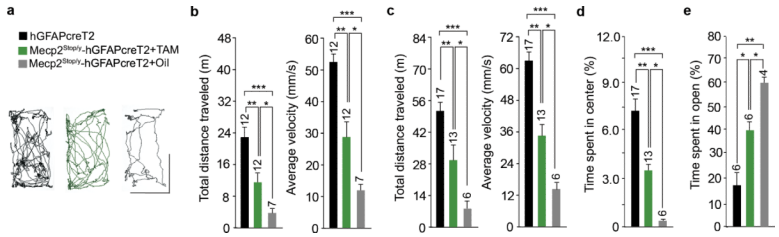

Figure 2.

a, Representative activity in a home-cage-like setting. Duration interval, 5 min. Scale bars indicate 7 inches. **b**, Locomotor activity histograms in a home-cage-like setting. Duration interval, 10 min. **c**, Locomotor activity histograms in an open field. Duration, 20 min. **d**, Time spent in centre of an open field. **e**, Time spent in open portions of an elevated zero maze. Mice aged 3-4 months. **P* < 0.05, ***P* < 0.01, ****P* < 0.001. All error bars indicate s.e.m. The number of mice analysed is indicated above each bar. **b**-**e**, Genotypes as in **a**.

NIH-PA Author Manuscript NIH-PA Author Manuscript NIH-PA Author Manuscript

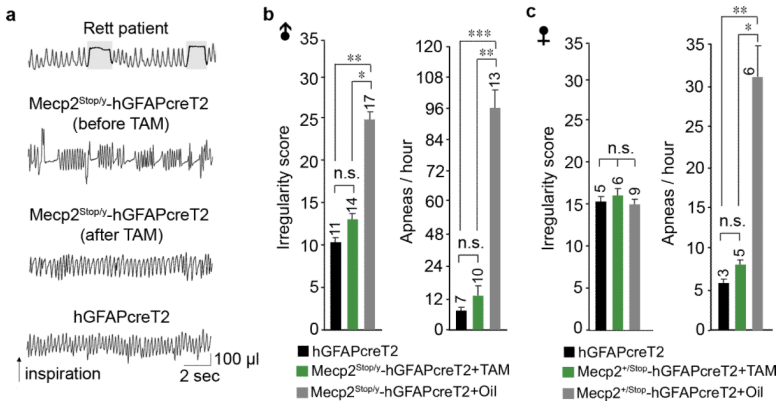

Figure 3.

a, Representative plethysmographic recordings from a female RTT patient (modified from ref. 22) and an *Mecp2*$^{Stop/y}$*-hGFAPcreT2* mouse and control. The two middle traces are from the same *Mecp2*$^{Stop/y}$*-hGFAPcreT2* mouse before and 62 days after TAM treatment (Supplementary Fig. 7c, trace 3). **b**, Respiratory irregularity scores and apnoea rates for male mice. **c**, Same as in **b** except for female mice. Mice showing at least 1 apnoea per hour were considered for apnoea rates. All error bars indicate s.e.m. **P* < 0.05, ***P* < 0.01, ****P* < 0.001. NS, not significant. The number of mice analysed is indicated above each bar.

NIH-PA Author Manuscript NIH-PA Author Manuscript NIH-PA Author Manuscript

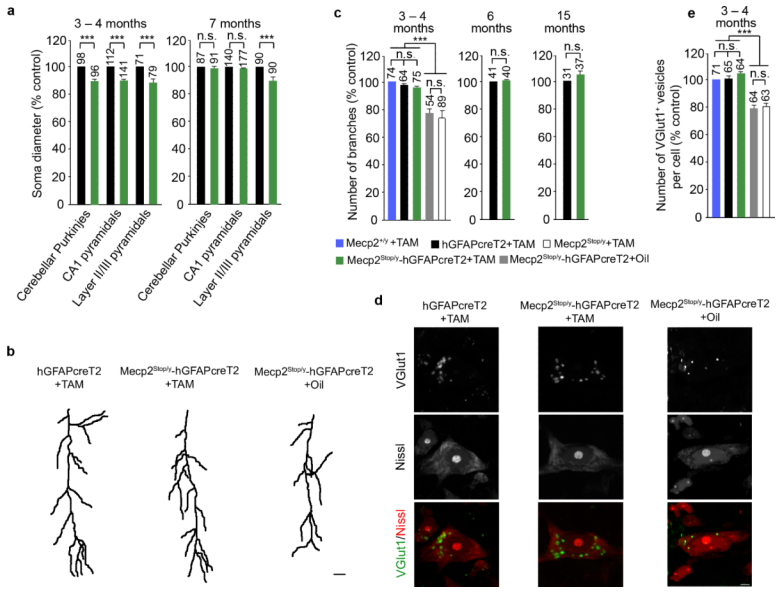

Figure 4.

a, Somal diameters of indicated neurons. Control, *hGFAPcreT2* + TAM. **b**, Representative traces of silver-impregnated hippocampal CA1 neurons from male mice aged 3-4 months. **c**, Number of silver-impregnated CA1 apical branches in male mice. Control, $Mecp2^{+/y}$ + TAM. **d**, Representative images of Nissl-stained neurons immunolabelled for VGLUT1 from medulla oblongata. Scale bar: 10 μm (**b**); 2 μm (**d**). **e**, Number of $VGLUT1^{+}$ puncta associated with neuronal cell bodies from the medulla oblongata. All error bars indicate s.e.m. ***$P < 0.001$. NS, not significant. The number of analysed cells is indicated above each bar.

NIH-PA Author Manuscript NIH-PA Author Manuscript NIH-PA Author Manuscript